

Med-CRAFT: Automated Construction of Interpretable and Multi-Hop Video Workloads via Knowledge Graph Traversal

Shenxi Liu
Beijing Institute of Technology
Beijing, China
liushenxi@bit.edu.cn

Kan Li
Beijing Institute of Technology
Beijing, China
likan@bit.edu.cn

Mingyang Zhao
The Hong Kong Polytechnic
University
Hongkong, China
mingyang.zhao@polyu.edu.hk

Yuhang Tian
Beijing Institute of Technology
Beijing, China
tianyuhang@bit.edu.cn

Shoujun Zhou
Shenzhen Institute of Advanced
Technology, Chinese Academy of
Sciences
Shenzhen, China
sj.zhou@siat.ac.cn

Bin Li
Shenzhen Institute of Advanced
Technology, Chinese Academy of
Sciences
Shenzhen, China
b.li2@siat.ac.cn

ABSTRACT

The scarcity of high-quality, logically annotated video datasets remains a primary bottleneck in advancing Multi-Modal Large Language Models (MLLMs) for the medical domain. Traditional manual annotation is prohibitively expensive and non-scalable, while existing synthetic methods often suffer from stochastic hallucinations and a lack of logical interpretability. To address these challenges, we introduce **Med-CRAFT**, a novel neuro-symbolic data engineering framework that formalizes benchmark synthesis as a deterministic graph traversal process. Unlike black-box generative approaches, Med-CRAFT extracts structured visual primitives (e.g., surgical instruments, anatomical boundaries) from raw video streams and instantiates them into a dynamic Spatiotemporal Knowledge Graph. By anchoring query generation to valid paths within this graph, we enforce a rigorous Chain-of-Thought (CoT) provenance for every synthesized benchmark item. We instantiate this pipeline to produce M³-Med-Auto, a large-scale medical video reasoning benchmark exhibiting fine-grained temporal selectivity and multi-hop logical complexity. Comprehensive evaluations demonstrate that our automated pipeline generates query workloads with complexity comparable to expert-curated datasets. Furthermore, a logic alignment analysis reveals a high correlation between the prescribed graph topology and the reasoning steps of state-of-the-art MLLMs, validating the system’s capability to encode verifiable logic into visual-linguistic benchmarks. This work paves the way for scalable, low-cost construction of robust evaluation protocols in critical domains.

PVLDB Artifact Availability:

The source code, data, and/or other artifacts have been made available at <https://Med-M3-Dataset.github.io/>.

1 INTRODUCTION

The exponential growth of unstructured video data in specialized domains, particularly healthcare, has precipitated a critical need for benchmarks capable of evaluating complex analytical workloads. Unlike general-purpose retrieval tasks that prioritize coarse-grained object detection (e.g., "find a car"), medical instructional analysis

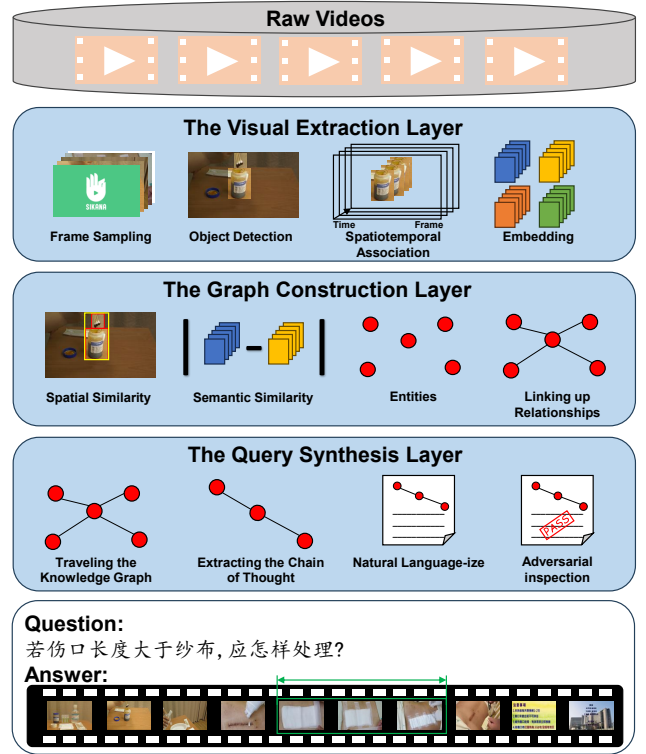


Figure 1: The basic structure of Med-CRAFT, including visual extraction layer (pixel-level), graph construction layer (semantic-level), query synthesis layer (logic-level)

requires distinct procedural precision, involving fine-grained entities and rigorous causal logic. Consequently, querying such data necessitates not only grounding fine-grained actions (e.g., specific surgical maneuvers) but also reasoning over complex, multi-hop temporal dependencies (e.g., "identify steps immediately following iodine application"). However, current methodologies for constructing video query benchmarks exhibit significant limitations

when applied to domains requiring strict logical coherence. First, expert-driven manual annotation, while ensuring high quality, incurs prohibitive costs and lacks the scalability required to generate the massive datasets needed for evaluating modern data-intensive systems. Second, simulation-based synthesis, though effective for physically rigid scenarios like traffic, fails to model the stochastic biological complexity and diverse operational nuances inherent in real-world medical procedures. Third, generative approaches utilizing Large Language Models (LLMs) often depend excessively on textual modalities (e.g., subtitles), resulting in a "semantic gap" where generated queries lack precise grounding in fine-grained visual primitives. Furthermore, the "black-box" nature of end-to-end generation introduces non-deterministic hallucinations and lacks the provenance tracking necessary to diagnose query execution failures, rendering such benchmarks unreliable for rigorous system evaluation. To address these challenges, we propose **Med-CRAFT (Medical Cross-modal Reasoning And Fine-grained Tracking)**, a novel automated framework that synthesizes complex queries by constructing and traversing a fine-grained, cross-modal Knowledge Graph (KG) derived from raw video data. Rather than relying on opaque inference, our approach explicitly models procedural logic as structured graph paths, where nodes encapsulate fine-grained visual concepts and edges enforce strict logical or temporal constraints. By programmatically deriving query-answer pairs from these validated graph structures, we ensure that every generated benchmark instance possesses a deterministic logic chain and verifiable visual grounding. We instantiate this pipeline to construct M^3 -Med-Auto, a large-scale, fine-grained medical video QA dataset. Extensive experimental evaluation demonstrates that our KG-guided tool-chain significantly optimizes the cost-quality trade-off. Specifically, Med-CRAFT generates datasets featuring fine-grained alignment and multi-hop reasoning challenges that rival expert annotation in fidelity, while achieving full lineage transparency at a fraction of the cost. Crucially, the pipeline enables rapid workload scalability, facilitating the generation of massive, diverse query sets designed to expose the reasoning bottlenecks of state-of-the-art video understanding systems.

2 RELATED WORK

We review existing approaches for constructing video query benchmarks, categorizing them into three primary workflows: manual annotation, (M)LLM-based generation, and simulation-based synthesis.

2.1 Manual Annotation Pipelines

Early benchmarks primarily rely on crowdsourcing or expert annotation to ensure high semantic quality. A representative work, MedVidQA [1], proposes a pipeline that retrieves medical instructional videos based on textual queries from trusted health resources (e.g., WikiHow) and employs human annotators to manually label the start and end timestamps of visual segments answering specific questions. While manual annotation ensures the authenticity of the video source, it suffers from prohibitive scalability costs. As noted in a similar manual annotation work, M^3 -Med [2], ensuring high-quality temporal localization requires rigorous expert verification, making it impossible to scale to the millions of training examples

needed for modern deep learning models. Furthermore, human annotators often struggle to consistently define precise boundaries for fine-grained actions, leading to subjective bias in the ground truth.

2.2 (M)LLM-based Automated Generation

To mitigate the scalability constraints inherent in manual annotation, recent research has pivoted towards utilizing Large Language Models (LLMs) or Multi-modal Large Language Models (MLLMs) for automated dataset synthesis. For instance, HealthVidQA [3] proposes a framework that leverages domain-adapted LLMs to derive question-answer pairs directly from Automatic Speech Recognition (ASR) transcripts, enabling the construction of large-scale datasets with minimal human intervention. However, the primary limitation of such text-centric approaches is the inherent "modality gap": by synthesizing queries based solely on textual metadata rather than raw visual signals, these methods frequently fail to ensure precise visual grounding. To address this misalignment, recent efforts like ShareGPT4Video [4] employ MLLMs, such as GPT-4V, to generate queries directly from sampled video frames, aiming to better align textual inquiries with visual content. Nevertheless, these end-to-end generative models operate as probabilistic "black boxes," making them inherently prone to hallucinations—a critical vulnerability in high-stakes medical domains where data integrity is paramount. Specifically, such models may hallucinate entities not present in the visual stream or synthesize procedural sequences that violate strict medical logic. Correcting these errors necessitates complex, unreliable post-hoc filtering pipelines, thereby undermining the efficiency and trustworthiness of the automated generation process.

2.3 Simulation-based Synthesis

A third paradigm circumvents the manual annotation bottleneck entirely by leveraging graphics engines for programmatic data synthesis. Pioneering works such as CLEVR [5] established this paradigm, utilizing physics engines to construct structured visual reasoning benchmarks. The distinct advantage of this approach lies in its access to the underlying simulation state—such as precise object coordinates and velocities—which guarantees absolute ground truth accuracy during dataset construction. This bypasses the noise and ambiguity inherent in extracting metadata from raw, "second-hand" video feeds. Subsequently, this paradigm has been scaled to the temporal dimension, extending from static images to dynamic video. Notable frameworks like VisualRoad [6] leverage high-fidelity graphics engines (e.g., Unity) to render complex traffic scenarios, enabling the automated construction of large-scale synthetic video benchmarks for autonomous driving. However, while highly effective for rigid-body domains such as autonomous driving, this methodology encounters prohibitive feasibility barriers within the medical context. Accurately modeling the deformable dynamics of human tissue and the fluid complexity of surgical interventions requires computational resources that scale non-linearly with realism. Consequently, synthetic medical datasets frequently suffer from a severe "Sim-to-Real" domain shift. To resolve these dichotomies, our work proposes a hybrid framework that synthesizes the strengths of real-world data capture and structured logic generation. We leverage real-world video data to obviate the Sim-to-Real

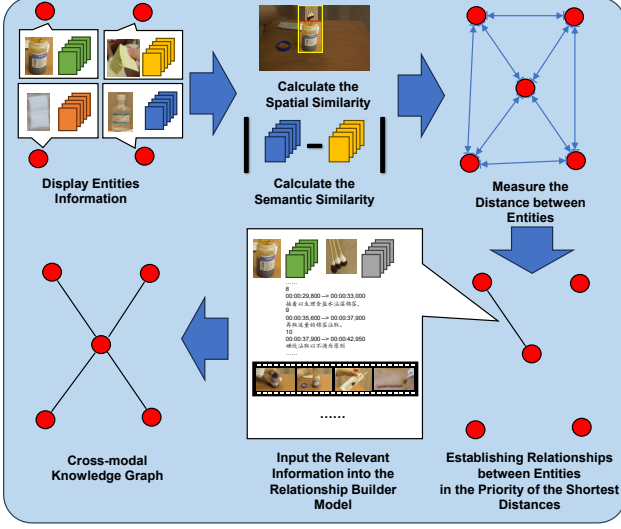


Figure 3: Dynamic Knowledge Graph Construction: Instantiating a symbolic graph where nodes represent visual entities and edges encode temporal interactions.

The **comprehensive affinity score** is then derived via a gated fusion mechanism:

$$P(v_i, v_j) = \mathbb{I}[S_{\text{semantic}} > \tau_{\text{sem}}] \cdot (\alpha \cdot S_{\text{semantic}} + (1 - \alpha) \cdot S_{\text{spatial}}) \quad (3)$$

where $\mathbb{I}[\cdot]$ is an indicator function serving as a semantic consistency gate (implemented via thresholding or ReLU in practice), and α is a balancing hyperparameter.

Finally, we employ the Hungarian Algorithm to solve the global assignment problem based on affinity matrix P . Matched primitives are linked to form a **Spatiotemporal Tubelet**, denoted as $\mathcal{T}_k = \{v_k^{(t_1)}, v_k^{(t_2)}, \dots, v_k^{(t_m)}\}$, representing the continuous trajectory of the k -th entity.

3.2 Neuro-Symbolic Knowledge Graph Construction

In this phase, we elevate the representation from pixel-level trajectories to a semantic Knowledge Graph $\mathcal{G} = (\mathcal{V}, \mathcal{E})$. Each spatiotemporal tubelet \mathcal{T}_k derived in the previous step is instantiated as a unique entity node $e_k \in \mathcal{V}$. The structure of this component is shown in the Fig. 3.

Entity Relationship Modeling. To discover latent relationships between entities (e.g., *Instrument A cuts Tissue B*), we evaluate pairwise affinities across the temporal dimension. We employ Video-CLIP [9] to encode the aggregated video segments of each tubelet, yielding global semantic embeddings. The relationship extraction logic considers both **long-term semantic interaction** and **instantaneous spatial proximity**.

We define the **Spatio-Temporal Overlap Score** (S_{st}) to capture physical interactions (e.g., touching, cutting) by averaging the GIoU

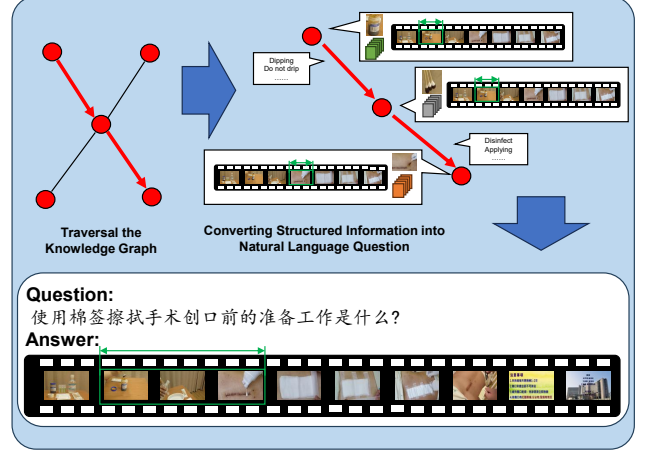


Figure 4: Logic-Guided Query Synthesis: Generating complex, multi-hop QA pairs via deterministic graph traversal, ensuring strict alignment between visual evidence and textual logic.

over the co-existent frames T_{overlap} :

$$S_{st}(\mathcal{T}_k, \mathcal{T}_q) = \frac{1}{|T_{\text{overlap}}|} \sum_{t \in T_{\text{overlap}}} \text{GIoU}(b_k^{(t)}, b_q^{(t)}) \quad (4)$$

Simultaneously, to capture correlated motion patterns (e.g., an instrument following a specific path relative to an organ), we calculate the **Trajectory Similarity** (S_{traj}) using Dynamic Time Warping (DTW). We convert the DTW distance into a similarity score via an exponential kernel:

$$S_{\text{traj}}(\mathcal{T}_k, \mathcal{T}_q) = \exp(-\gamma \cdot \text{DTW}(\mathbf{c}_k, \mathbf{c}_q)) \quad (5)$$

where \mathbf{c} denotes the sequence of centroid coordinates of the bounding boxes, and γ is a decay hyperparameter controlling sensitivity.

The **Connection Priority Score** is computed by fusing the semantic cosine similarity (S_{sem}) with the motion metrics:

$$P_{\text{edge}}(\mathcal{T}_k, \mathcal{T}_q) = \sigma(S_{\text{sem}}) \cdot (\beta S_{st} + (1 - \beta) S_{\text{traj}}) \quad (6)$$

Pairs with P_{edge} exceeding a confidence threshold are candidate edges. To resolve the specific semantic predicate of the edge (e.g., *grasps*, *cauterizes*), we feed the visual crops and metadata of the interacting tubelets into an MLLM (Qwen3-VL [10]). The MLLM acts as a neuro-symbolic reasoned, assigning explicit relationship labels to edges, thereby completing the construction of \mathcal{G} .

3.3 Logic-Driven Query Synthesis and Validation

Once the Knowledge Graph \mathcal{G} is constructed, we transform the benchmark generation task into a path traversal problem. This ensures that every generated question is grounded in a verifiable logical chain. The structure of this component is shown in the Fig. 4.

Path-Based Query Synthesis. We employ a Depth-First Search (DFS) algorithm to traverse \mathcal{G} , identifying directed paths $p = (e_{\text{start}}, r_1, e_1, \dots, e_{\text{end}})$. Each path represents a distinct causal or

temporal sequence of medical events. For each extracted path, we retrieve the visual context and metadata of the nodes and edges. These structured signals are input into a generative MLLM (Qwen3-VL[10]) with a specialized prompt strategy:

- (1) **Input:** The structured path information (e.g., *cotton swabs infiltration* \rightarrow *iodine smear* \rightarrow *skin*).
- (2) **Instruction:** Synthesize a natural language question where e_{start} serves as the premise and the temporal segment of e_{end} serves as the answer.
- (3) **Constraint:** The reasoning process must strictly follow the path topology.

Adversarial Validation Mechanism. To ensure the rigorosity of the medical logic, we implement a critic-based validation loop. A separate, more powerful MLLM (GPT-4V[11]) acts as an independent "Judge." It receives generated questions and original videos, and attempts to score and rank the questions by quality; only qualified questions are included in the dataset. This adversarial filtering minimizes the inclusion of ambiguous or unanswerable queries.

4 DATASET PROFILING: M³-MED-AUTO AND EXPERIMENTAL EVALUATION

In this section, we present M³-Med-Auto, a re-annotated instantiation of the M³-Med[2] corpus generated via our proposed pipeline. This dataset serves not only as a standalone resource but as a proof-of-concept validation for the efficacy of our Knowledge-Graph-guided synthesis methodology. Adopting the taxonomy established in M³-Med, we categorize queries based on their topological complexity within the knowledge graph: queries corresponding to single-hop traversals are designated as **Simple Questions**, while those necessitating multi-hop reasoning paths are classified as **Complex Questions**. We systematically characterize the statistical and semantic properties of each category to ensure alignment with existing benchmarks.

While M³-Med-Auto is derived from a curated selection of high-fidelity medical instructional videos, our primary objective extends beyond the release of a static data artifact; rather, we aim to validate the robust generative capabilities and architectural soundness of the underlying system. Specifically, we seek to empirically demonstrate that our automated pipeline synthesizes query workloads exhibiting fine-grained temporal selectivity, rigorous multi-hop logical complexity, and precise visual-semantic alignment—metrics that we show to be comparable to, or exceeding, those of manually curated expert benchmarks. Furthermore, through a structural analysis of the generated query graphs, we highlight the pipeline’s potential for horizontal scalability. This capability paves the way for generating large-scale neuro-symbolic workloads where the marginal cost of annotation approaches zero, decoupling dataset scale from human labor constraints.

4.1 Statistical Profiling of M³-Med-Auto

To quantitatively benchmark the difficulty and granularity of M³-Med-Auto against existing corpora, we introduce two rigorous statistical metrics: (1) the Temporal Selectivity Ratio, defined as the duration of the ground-truth answer segment relative to the full

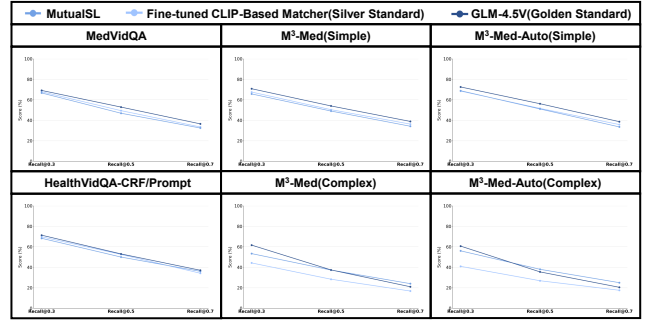


Figure 5: In the results of Task 1, we compare our retrieval performance with state-of-the-art baselines and control groups. Our method significantly outperforms existing datasets on challenging tasks, especially in scenarios requiring precise time alignment.

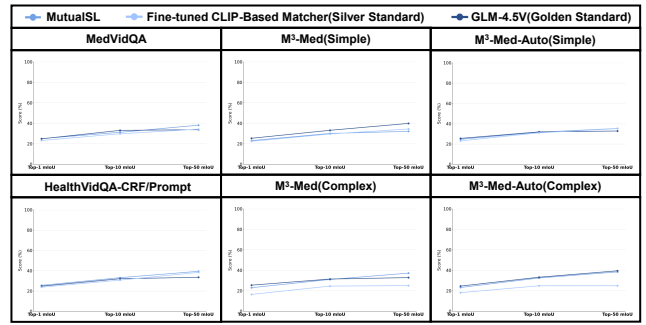


Figure 6: In the results of Task 2, we compare our retrieval performance with state-of-the-art baselines and control groups. Our method also demonstrates significant advantages on challenging existing datasets.

video length; and (2) the Semantic Contextual Confusion, measured by the cosine similarity between the answer segment and its adjacent non-answer temporal neighborhoods using Video-CLIP[9] embeddings.

Figs. 5,6 presents a comparative statistical summary of M³-Med-Auto versus prominent baselines, highlighting metrics on temporal granularity and semantic ambiguity.

As evidenced by the empirical data, M³-Med-Auto exhibits a significantly lower temporal selectivity ratio compared to peer datasets, necessitating highly precise temporal regression capabilities. Furthermore, the elevated Semantic Contextual Confusion scores indicate that our answer segments are semantically indistinguishable from their immediate temporal context without deep logical reasoning. Together, these characteristics underscore the dataset’s suitability as a challenging testbed for fine-grained, logic-dependent video localization.

4.2 Benchmarking Reasoning Difficulty

To strictly evaluate the logical reasoning capabilities of visual-language models on M³-Med-Auto, we adhere to the rigorous evaluation protocols established in M³-Med, formalizing the assessment

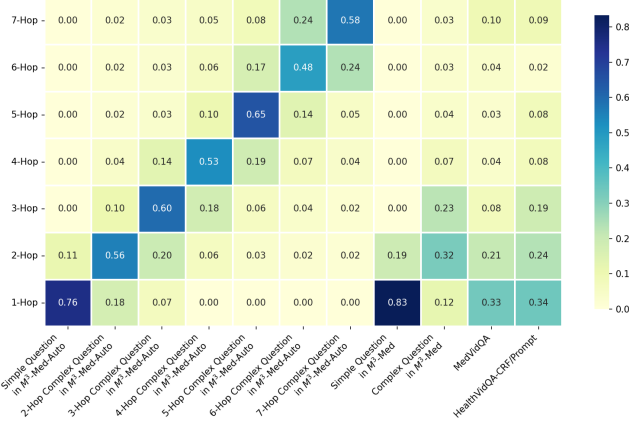


Figure 7: Alignment analysis between the designed logic depth and the Golden Standard. The heatmap visualizes the distribution of actual reasoning hops (Y-axis) for questions generated with specific intended complexities (X-axis). The strong diagonal dominance within the M³-Med-Auto block confirms the structural consistency of our pipeline: questions designed to require N hops of reasoning are correctly verified as N -hop queries in the Golden Standard. This demonstrates that our neuro-symbolic engine can synthesize benchmarks with precise control over logic complexity, avoiding the semantic drift often seen in black-box generation.

into two distinct tasks: Temporal Answer Grounding in Single Video and Temporal Answer Grounding in Video Corpus.

Task 1: Temporal Answer Grounding in Single Video (TAGSV)

Problem Definition. Given a natural language query Q and a reference medical video V , the objective is to localize the specific temporal segment $T^* = [t_{start}^*, t_{end}^*]$ that semantically answers Q .

Metric Formulation. Let T_i denote the predicted interval and T_i^* the ground-truth interval for the i -th query. We quantify the localization accuracy using the Temporal Intersection over Union (IoU):

$$\text{IoU}(T_i, T_i^*) = \frac{\text{duration}(T_i \cap T_i^*)}{\text{duration}(T_i \cup T_i^*)} \quad (7)$$

Performance is aggregated using **Recall@ τ** (the percentage of queries where IoU exceeds a threshold $\tau \in \{0.3, 0.5, 0.7\}$):

$$\text{R@}\tau = \frac{1}{N} \sum_{i=1}^N \mathbb{I}[\text{IoU}(T_i, T_i^*) \geq \tau] \quad (8)$$

where N is the total number of samples and $\mathbb{I}[\cdot]$ is the indicator function.

Task 2: Temporal Answer Grounding in Video Corpus (TAGVC)

Problem Definition. This task extends TAGSV to a retrieval setting. Given a query Q and a video corpus $\mathcal{V} = \{V_1, \dots, V_M\}$, the model must identify the target video V^* and localize the evidence segment T^* . The model outputs a ranked list of $K = 50$ hypotheses $\{(V_{i,j}, T_{i,j})\}_{j=1}^K$, ordered by confidence.

Metric Formulation. We define a scoring function $S_{i,j}$ that penalizes incorrect video retrieval:

$$S_{i,j} = \mathbb{I}[V_{i,j} = V_i^*] \cdot \text{tIoU}(T_{i,j}, T_i^*) \quad (9)$$

To evaluate the combined retrieval and localization performance, we employ the **Top- K mIoU** metric, which considers the best-localized hypothesis within the top- K retrieved candidates:

$$\text{Top-}K \text{ mIoU} = \frac{1}{N} \sum_{i=1}^N \max_{j \leq K} S_{i,j} \quad (10)$$

We report results for $K \in \{1, 10, 50\}$.

Baselines and Comparative Analysis To benchmark the complexity of M³-Med-Auto, we evaluate three distinct tiers of solvers:

- **Supervised Specialist:** MutualSL [12], a baseline trained specifically on medical video grounding tasks.
- **Heuristic Baseline** (Silver Standard): A fine-tuned CLIP-based matcher, representing a purely semantic approach without structural reasoning capabilities.
- **Chain-of-Thought Oracle** (Golden Standard): GLM-4.5V [13], a state-of-the-art MLLM equipped with high-resolution vision and long-context window. We utilize a specific "Step-by-Step" prompting strategy to elicit explicit reasoning chains, serving as an upper-bound proxy for reasoning capability.

Beyond standard metrics, we conduct a **Logic Alignment Analysis** for the Oracle baseline. We quantify the correlation between the *Prescribed Hop Count* (defined by our generation pipeline) and the *Inferred Hop Count* (the number of reasoning steps actually emitted by GLM-4.5V).

Experimental Results and Observations The experimental outcomes validate following critical hypotheses regarding M³-Med-Auto:

- **Human-Parity Complexity:** The performance gap between the Supervised Specialist and the Oracle indicates that our synthesized queries achieve a level of complexity comparable to expert-curated problems, necessitating advanced reasoning beyond simple pattern matching.
- **Distinguishability of Logic:** The performance stratification between Simple and Complex queries is pronounced across all models. Notably, the CLIP-based Heuristic fails significantly on Complex queries (Multi-hop), whereas the CoT Oracle maintains robustness.
- **Neuro-Symbolic Alignment:** As illustrated in the alignment heatmap (Fig. 7), there exists a strong positive correlation between the pipeline’s prescribed complexity and the Oracle’s reasoning depth. This confirms that our automated pipeline successfully encodes valid, deterministically solvable multi-hop logic into the generated benchmarks.

5 CONCLUSION AND FUTURE WORK

In this paper, we presented Med-CRAFT, a systematic framework that reimagines medical video benchmark construction not as a labor-intensive manual task, but as a scalable, logic-driven engineering process. By bridging the gap between pixel-level visual extraction and symbolic knowledge representation, our pipeline successfully mitigates the hallucination risks inherent in purely

generative approaches. The resulting dataset, M³-Med-Auto, serves as a rigorous testbed for next-generation MLLMs, offering precise spatiotemporal grounding and verifiable multi-hop reasoning challenges that were previously attainable only through expert curation. Our empirical analysis confirms that the logical structures encoded by our pipeline effectively translate into the cognitive reasoning chains of SOTA models, proving that synthetic data can achieve both high fidelity and deep logic.

5.1 Future Work

We envision several promising directions to extend this neuro-symbolic architecture:

Cross-Modal Knowledge Expansion: We plan to integrate disparate medical modalities (e.g., CT scans, electronic health records) into the knowledge graph, evolving the benchmark from visual perception to comprehensive clinical diagnosis.

Active Learning Feedback Loop: We aim to close the loop by using the performance metrics of evaluated models to automatically identify "weak paths" in the knowledge graph, guiding the pipeline to generate harder, adversarial training samples for continuous model improvement.

Privacy-Preserving Federated Synthesis: Given the sensitivity of medical data, we intend to explore federated execution of our pipeline, allowing hospitals to generate standardized benchmarks locally without sharing raw patient video data.

ACKNOWLEDGMENTS

This work was supported by National Natural Science Foundation of China (Nos. 4222037 and L181010), and Sanming Project of Medicine in Shenzhen (No. SZZYSM202311002).

REFERENCES

- [1] D. Gupta, K. Attal, and D. Demner-Fushman. A dataset for medical instructional video classification and question answering. *Scientific Data*, 10(1):158, Mar 2023.
- [2] Shenxi Liu, Kan Li, Mingyang Zhao, Yuhang Tian, Bin Li, Shoujun Zhou, Hongliang Li, and Fuxia Yang. M³-Med: A Benchmark for Multi-lingual, Multi-modal, and Multi-hop Reasoning in Medical Instructional Video Understanding. *arXiv e-prints*, page arXiv:2507.04289, July 2025.
- [3] Deepak Gupta, Kush Attal, and Dina Demner-Fushman. Towards answering health-related questions from medical videos: Datasets and approaches. In Nicoletta Calzolari, Min-Yen Kan, Veronique Hoste, Alessandro Lenci, Sakriani Sakti, and Nianwen Xue, editors, *Proceedings of the 2024 Joint International Conference on Computational Linguistics, Language Resources and Evaluation (LREC-COLING 2024)*, pages 16399–16411, Torino, Italia, May 2024. ELRA and ICCL.
- [4] Lin Chen, Xilin Wei, Jinsong Li, Xiaoyi Dong, Pan Zhang, Yuhang Zang, Zehui Chen, Haodong Duan, Bin Lin, Zhenyu Tang, Li Yuan, Yu Qiao, Dahua Lin, Feng Zhao, and Jiaqi Wang. Sharegpt4video: improving video understanding and generation with better captions. In *Proceedings of the 38th International Conference on Neural Information Processing Systems*, NIPS ’24, Red Hook, NY, USA, 2024. Curran Associates Inc.
- [5] Justin Johnson, Bharath Hariharan, Laurens van der Maaten, Li Fei-Fei, C. Lawrence Zitnick, and Ross Girshick. Clevr: A diagnostic dataset for compositional language and elementary visual reasoning. In *Proceedings of the IEEE Conference on Computer Vision and Pattern Recognition (CVPR)*, July 2017.
- [6] Brandon Haynes, Amrita Mazumdar, Magdalena Balazinska, Luis Ceze, and Alvin Cheung. Visual road: A video data management benchmark. In *Proceedings of the 2019 International Conference on Management of Data*, SIGMOD ’19, page 972–987, New York, NY, USA, 2019. Association for Computing Machinery.
- [7] Shilong Liu, Zhaoyang Zeng, Tianhe Ren, Feng Li, Hao Zhang, Jie Yang, Qing Jiang, Chunyuan Li, Jianwei Yang, Hang Su, Jun Zhu, and Lei Zhang. Grounding dino: Marrying dino with grounded pre-training for open-set object detection. In Aleks Leonidis, Elisa Ricci, Stefan Roth, Olga Russakovsky, Torsten Sattler, and Gül Varol, editors, *Computer Vision – ECCV 2024*, pages 38–55, Cham, 2025. Springer Nature Switzerland.
- [8] Alec Radford, Jong Wook Kim, Chris Hallacy, Aditya Ramesh, Gabriel Goh, Sandhini Agarwal, Girish Sastry, Amanda Askell, Pamela Mishkin, Jack Clark, Gretchen Krueger, and Ilya Sutskever. Learning transferable visual models from natural language supervision. In *International Conference on Machine Learning*, 2021.
- [9] Jiapeng Wang, Chengyu Wang, Kunzhe Huang, Jun Huang, and Lianwen Jin. Videoclip-xl: Advancing long description understanding for video clip models, 2024.
- [10] Shuai Bai, Yuxuan Cai, Ruizhe Chen, Keqin Chen, Xionghui Chen, Zesen Cheng, Lianghao Deng, Wei Ding, Chang Gao, Chunjiang Ge, Wenbin Ge, Zhifang Guo, Qidong Huang, Jie Huang, Fei Huang, Binyuan Hui, Shutong Jiang, Zhaohai Li, Mingsheng Li, Mei Li, Kaixin Li, Zicheng Lin, Junyang Lin, Xuejing Liu, Jiawei Liu, Chenglong Liu, Yang Liu, Dayiheng Liu, Shixuan Liu, Dunjie Lu, Ruilin Luo, Chenxu Lv, Rui Men, Lingchen Meng, Xuancheng Ren, Xingzhang Ren, Sibo Song, Yuchong Sun, Jun Tang, Jianhong Tu, Jianqiang Wan, Peng Wang, Pengfei Wang, Qiyue Wang, Yuxuan Wang, Tianbao Xie, Yiheng Xu, Haiyang Xu, Jin Xu, Zhibo Yang, Mingkun Yang, Jianxin Yang, An Yang, Bowen Yu, Fei Zhang, Hang Zhang, Xi Zhang, Bo Zheng, Humen Zhong, Jingren Zhou, Fan Zhou, Jing Zhou, Yuanzhi Zhu, and Ke Zhu. Qwen3-VL Technical Report. *arXiv e-prints*, page arXiv:2511.21631, November 2025.
- [11] OpenAI, Josh Achiam, Steven Adler, Sandhini Agarwal, Lama Ahmad, Ilge Akkaya, Florencia Leoni Aleman, Diogo Almeida, Janko Altmenschmidt, Sam Altman, Shyamal Anadkat, Red Adella, Igor Babuschkin, Suchir Balaji, Valerie Balcom, Paul Bahtescu, Haiming Bao, Mohammad Bavarian, Jeff Belgum, Irwan Bello, Jake Berdine, Gabriel Bernadett-Shapiro, Christopher Berner, Lenny Bogdonoff, Oleg Boiko, Madeline Boyd, Anna-Luisa Brakman, Greg Brockman, Tim Brooks, Miles Brundage, Kevin Button, Trevor Cai, Rosie Campbell, Andrew Cann, Britany Carey, Chelsea Carlson, Rory Carmichael, Brooke Chan, Che Chang, Fotis Chantzis, Derek Chen, Sully Chen, Ruby Chen, Jason Chen, Mark Chen, Ben Chess, Chester Cho, Casey Chu, Hyung Won Chung, Dave Cummings, Jeremiah Currier, Yunxing Dai, Cory Decareaux, Thomas Degry, Noah Deutsch, Damien Deville, Arka Dhar, David Dohan, Steve Dowling, Sheila Dunning, Adrien Ecoffet, Atty Eleti, Tyna Eloundou, David Farhi, Liam Fedus, Niko Felix, Simón Posada Fishman, Juston Forte, Isabella Fulford, Leo Gao, Elie Georges, Christian Gibson, Vik Goel, Tarun Gogineni, Gabriel Goh, Rapha Gontijo-Lopes, Jonathan Gordon, Morgan Grafstein, Scott Gray, Ryan Greene, Joshua Gross, Shixiang Shane Gu, Yufei Guo, Chris Hallacy, Jesse Han, Jeff Harris, Yuchen He, Mike Heaton, Johannes Heidecke, Chris Hesse, Alan Hickey, Wade Hickey, Peter Hoeschele, Brandon Houghton, Kenny Hsu, Shengli Hu, Xin Hu, Joost Huizinga, Shantanu Jain, Shawn Jain, Joanne Jang, Angela Jiang, Roger Jiang, Haozhun Jin, Denny Jin, Shino Jomoto, Billie Jonn, Heewoo Jun, Tomer Kaftan, Lukasz Kaiser, Ali Kamali, Ingmar Kanitscheider, Nitish Shirish Keskar, Tabarak Khan, Logan Kilpatrick, Jong Wook Kim, Christina Kim, Yongjik Kim, Jan Hendrik Kirchner, Jamie Kiros, Matt Knight, Daniel Kokotajlo, Lukasz Kondraciuk, Andrew Kondrich, Aris Konstantinidis, Kyle Kosic, Gretchen Krueger, Vishal Kuo, Michael Lampe, Ikai Lan, Teddy Lee, Jan Leike, Jade Leung, Daniel Levy, Chak Ming Li, Rachel Lim, Molly Lin, Stephanie Lin, Mateusz Litwin, Theresa Lopez, Ryan Lowe, Patricia Lue, Anna Makanju, Kim Malfacini, Sam Manning, Todor Markov, Yaniv Markovski, Bianca Martin, Katie Mayer, Andrew Mayne, Bob McGrew, Scott Mayer McKinney, Christine McLeavey, Paul McMillan, Jake McNeil, David Medina, Aalok Mehta, Jacob Menick, Luke Metz, Andrey Mishchenko, Pamela Mishkin, Vinnie Monaco, Evan Morikawa, Daniel Mossing, Tong Mu, Mira Murati, Oleg Murk, David Mély, Ashvin Nair, Reichihiro Nakano, Rajeev Nayak, Arvind Neelakantan, Richard Ngo, Hyeonwoo Noh, Long Ouyang, Cullen O’Keefe, Jakub Pachocki, Alex Paino, Joe Palermo, Ashley Pantuliano, Giambattista Parascandolo, Joel Parish, Emy Parparita, Alex Passos, Mikhail Pavlov, Andrew Peng, Adam Perelman, Filipe de Avila Belbute Peres, Michael Petrov, Henrique Ponde de Oliveira Pinto, Michael, Pokorny, Michelle Pokrass, Vitchyr H. Pong, Tolly Powell, Alethea Power, Boris Power, Elizabeth Proehl, Raul Puri, and Alec Radford. GPT-4 Technical Report. *arXiv e-prints*, page arXiv:2303.08774, March 2023.
- [12] Yixuan Weng and Bin Li. Visual answer localization with cross-modal mutual knowledge transfer. In *ICASSP 2023 - 2023 IEEE International Conference on Acoustics, Speech and Signal Processing (ICASSP)*, pages 1–5, 2023.
- [13] V Team, Wenyi Hong, Wenmeng Yu, Xiaotao Gu, Guo Wang, Guobing Gan, Haomiao Tang, Jiale Cheng, Ji Qi, Junhui Ji, Lihang Pan, Shuaiqi Duan, Weihang Wang, Yan Wang, Yean Cheng, Zehai He, Zhe Su, Zhen Yang, Ziyang Pan, Aohan Zeng, Baoxu Wang, Bin Chen, Boyan Shi, Changyu Pang, Chenhui Zhang, Da Yin, Fan Yang, Guoqing Chen, Jiazheng Xu, Jiale Zhu, Jiali Chen, Jing Chen, Jinhao Chen, Jinghao Lin, Jinjiang Wang, Junjie Chen, Leqi Lei, Letian Gong, Leyi Pan, Mingdao Liu, Mingde Xu, Mingzhi Zhang, Qinkai Zheng, Sheng Yang, Shi Zhong, Shiyu Huang, Shuyuan Zhao, Siyan Xue, Shangqin Tu, Shengbiao Meng, Tianshu Zhang, Tianwei Luo, Tianxiang Hao, Tianyu Tong, Wenkai Li, Wei Jia, Xiao Liu, Xiaohan Zhang, Xin Lyu, Xinyue Fan, Xuancheng Huang, Yanling Wang, Yadong Xue, Yanfeng Wang, Yanzi Wang, Yifan An, Yifan Du, Yiming Shi, Yiheng Huang, Yilin Niu, Yuan Wang, Yuanchang Yue, Yuchen Li, Yutao Zhang, Yuting Wang, Yu Wang, Yuxuan Zhang, Zhao Xue, Zhenyu Hou, Zhengxiao Du, Zihan Wang, Peng Zhang, Debing Liu, Bin Xu, Juanzi Li, Minlie Huang, Yuxiao

